Structure and Thermal Behavior of Layered Silver Perfluorocarboxylates

Seung Joon Lee, Sang Woo Han, Hyouk Jin Choi, and Kwan Kim*

Laboratory of Intelligent Interfaces, School of Chemistry and Molecular Engineering and Center for Molecular Catalysis, Seoul National University, Seoul 151-742, Korea

Received: February 1, 2002; In Final Form: May 16, 2002

The structure and thermal behavior of silver perfluorocarboxylates ($AgCO_2(CF_2)_nCF_3$, $n = 10$, 12, 14, and 16) have been investigated by using various analytical tools. The X-ray diffraction patterns were composed of a series of peaks that could be indexed to (0*k*0) reflections of a layered structure. The adjacent layers were presumed to overlap by as much as 94% of the terminal CF_3 groups. Diffuse reflectance infrared Fourier transform spectroscopy revealed that the binding state of the carboxylate group to silver was a bridging one. The thermal analyses indicated that a chain melting process commenced at ~560 K without any interim premelting event but the thermal decomposition reaction was followed immediately after the chain melting process. More importantly, the temperature at which the structural collapse occurred was found to be ~100 K higher than that in silver hydroalkanecarboxylate such as silver stearate. The enhanced thermal stability seemed to be associated with the high rigidity of the fluorocarbon chains. Perfluorocarbons are thus expected to be a promising organic moiety, endowing the organic/inorganic hybrid materials with high thermal stability.

1. Introduction

Self-assembled monolayers (SAMs) derived from fluorocarbon molecules have attracted much recent attention due to their very low surface energy (inertness) and extreme hydrophobicity (low wetting).[1−8] These characteristics are associated with the intrinsic nature of the fluorine atom. The F−F interactions mediated by the neighboring C−F bonds force the perfluorocarbon chain to adopt a helical conformation. Accordingly, the cross section of a perfluorocarbon chain becomes larger than that of a usual hydrocarbon chain; the van der Waals diameter of a fluorocarbon chain is 5.6 Å whereas that of a hydrocarbon chain is 4.2 Å.[1,9] In addition, perfluorocarbon chains are more rigid than analogous hydrocarbon chains,[10] and they are more resistant to oxidation and corrosion.[11] All of these factors contribute to the enhanced stability of the fluorocarbon materials against mechanical friction, thermal stress, and extreme acid/base conditions. Despite these merits, it is, however, difficult to fabricate fully perfluorinated SAMs on a solid substrate owing to the solvophobic (water/oil insoluble) nature of the perfluoro molecules. Most SAMs are thus fabricated using semifluorinated hydrocarbons. Studies on the monolayer structure,[12] thermal stability,[13] molecular dynamics,[14] and electrochemistry[15] of such SAMs have been conducted by several researchers as a function of the hydro- or fluorocarbon chain length.

As an analogue of 2D SAMs of thiols on Ag, considerable research interest has been focused recently on silver alkanethiolate ($AgS(CH_2)_nCH_3$) that consists of an infinite-sheet, two-dimensional, nonmolecular layered structure.[16] The alkyl chains in these systems possess a fully extended all-trans conformation. The silver alkanethiolate also manifests a phase transition to a micellar phase (hexagonal columnar mesophase) with a change of the coordination of Ag to thiolates from trigonal to diagonal upon melting.[16b]

Similarly to the silver alkanethiolate, silver alkanecarboxylate ($AgCO_2(CH_2)_nCH_3$) has also been reported to possess a layered structure.[17] Recently, we investigated the structure and thermal behavior of prototype $AgCO_2(CH_2)_nCH_3$, silver stearate.[18] The X-ray diffraction (XRD) pattern of silver stearate was found to be composed of a series of peaks that could be indexed to (0*k*0) reflections of a layered structure. The alkyl chains in silver stearate as prepared were in an all-trans conformational state with little or no significant gauche population. Upon heating the sample, structural changes took place particularly in two temperature regions.[18b] In the first region, the binding state of the carboxylate group changed from bridging to unidentate along with a disordering of the alkyl chains. Nonetheless, the layered structural motif was sustained in that temperature region, in sharp contrast to the case of silver alkanethiolate. The second structural change must be associated with the decomposition of silver stearate.

In conjunction with the above implications, we report herein the structure and thermal behavior of silver perfluorocarboxylates ($AgCO_2(CF_2)_nCF_3$, $n = 10$, 12, 14, and 16) obtained by means of scanning electron microscopy (SEM), X-ray diffraction (XRD), diffuse-reflectance infrared Fourier transform (DRIFT) spectroscopy, differential scanning calorimetry (DSC), and thermogravimetric analysis (TGA). The first concern was whether a layered structure would also be assumed for silver perfluorocarboxylate. The second concern was to know, if it consisted of a layered structure, how much the thermal characteristics of such a hybrid material would be affected by the incorporation of perfluorocarbons instead of hydrocarbons. The third concern was to obtain the physicochemical properties of 2D SAMs of perfluoro carboxylic acids on Ag indirectly from those of their 3D analogues, silver perfluorocarboxylates. We found that silver perfluorocarboxylates also had a layered structure, but in fact possessed substantially higher thermal stability than silver hydrocarboxylates. Considering the application prospects of organic/inorganic hybrid materials, the present observations will be invaluable because specific material properties, e.g., stiffness, strength, weight, nonlinear optical behavior, electrical conductivity, photochemical charge transfer, and

* Author to whom all correspondence should be addressed. Tel: +82-2-8806651. Fax: +82-2-8743704. E-mail: kwankim@plaza.snu.ac.kr.

10.1021/jp0255841 CCC: $22.00
Published on Web 07/04/2002

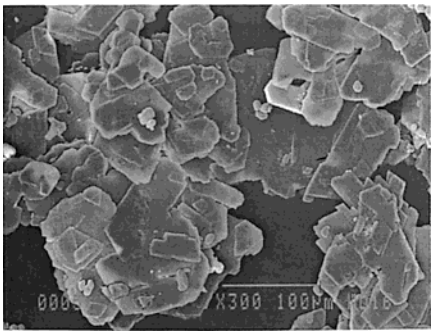

Figure 1. SEM image of AgF18.

ferromagnetism, can be manipulated by systematic variation of the structure and properties of the organic and inorganic constituents at the molecular level.[19]

2. Experimental Section

Preparation of Silver Perfluorocarboxylates. All perfluorocarboxylic acids (PFCAs, $CF_3(CF_2)_nCOOH$, $n = 10$ (F12), 12 (F14), 14 (F16), and 16 (F18); >95%) and hexafluorobenzene (HFB, >98%) were purchased from Fluorochem and used as received. Other chemicals, unless specified, were reagent grade. Glassware was cleaned using a KOH (1 kg) solution in 2-propanol (18 L) and water (1 L) mixture. Silver perfluorocarboxylates were prepared by the two-phase method. $AgNO_3$ (1 mmol) in 20 mL of methanol was added dropwise to an equimolar PFCA solution in 20 mL of HFB. After the mixture was stirred for 3 h, the white precipitates were filtered and then washed several times with HFB and hot chloroform. The resulting powders were dried in a vacuum for 3 h. To minimize light exposure, sample preparation was carried out using aluminum foil-wrapped flasks. These prepared samples, $AgCO_2(CF_2)_nCF_3$, will be called AgF12 ($n = 10$), AgF14 ($n = 12$), AgF16 ($n = 14$), and AgF18 ($n = 16$).

Characterization. SEM images of powdered samples were measured using a JSM 840-A scanning electron microscope at 20 kV. XRD patterns were obtained on a Philips X′PERT-MPD diffractometer for a 2θ range of 5−50° at an angular resolution of 0.02° using Cu Kα (1.5419 Å) radiation. The samples were spread on antireflection glass slides to give uniform films. Variable temperature XRD measurements were also carried out using the same diffractometer. Samples spread on Cr-coated Cu plates were heated to 573 K, within a temperature interval of 10 K. DSC and TGA were performed on TA instrument DSC-2010 and TGA-2050, respectively. These analyses were conducted in a nitrogen atmosphere (50 mL/min) between 298 and 773 K at a heating rate of 5 K/min. Infrared spectra were measured using a Bruker IFS 113v FT-IR spectrometer equipped with a globar light source and a liquid N_2-cooled wide-band mercury cadmium telluride detector. To record the DRIFT spectra, a diffuse reflection attachment (Harrick Model DRA-2CO) was fitted to the sampling compartment of the FT-IR spectrometer. The pure powdered sample was transferred to a 4-mm diameter cup without compression, and leveled by a gentle tap. Spectra were measured at a resolution of 4 cm^{-1} using previously scanned pure KBr as background.

3. Results and Discussion

Scanning electron micrographs (SEMs) of the silver perfluorocarboxylates ($AgCO_2(CF_2)_nCF_3$, $n = 10$, 12, 14, and 16) reveal that the samples have platelike morphology. A representative SEM image is shown in Figure 1 for AgF18. The platelets of

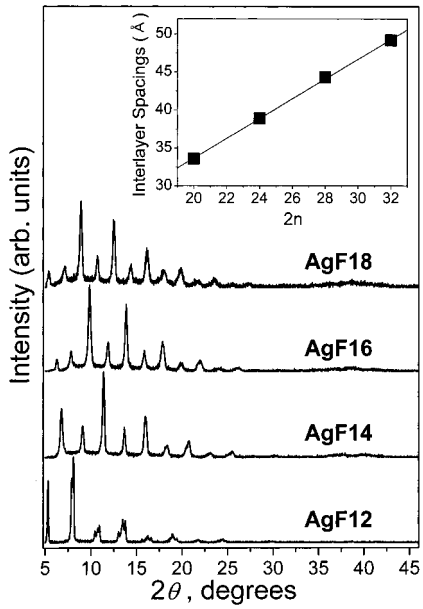

Figure 2. XRD patterns of $AgCO_2(CF_2)_nCF_3$. The interlayer spacing versus $2n$ is plotted in the inset; linear fit gives a slope of 1.30 ± 0.02 Å per $-CF_2-$ unit and Y-intercept of 7.65 ± 0.47 Å.

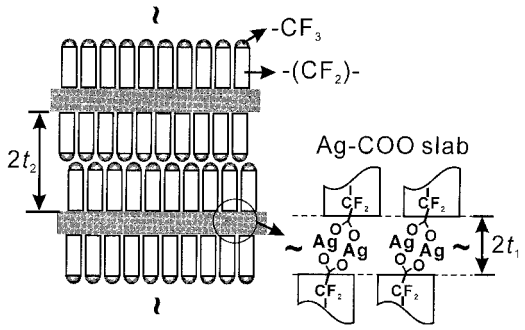

Figure 3. Schematic depiction of the layered structure of $AgCO_2(CF_2)_nCF_3$.

silver perfluorocarboxylates were identified as possessing a layered structure from the XRD data shown in Figure 2. All samples show a well-developed progression of intense diffraction patterns dominated by (0k0) reflections. These intense reflections can be interpreted in terms of three-dimensionally stacked silver carboxylate layers with a large interlayer lattice dimension,[17] as schematically drawn in Figure 3. The comparable XRD patterns of silver perfluorocarboxylates to silver hydrocarboxylates indicate that the layered structure is derived mostly from the Ag−COO bonds. This implies that each layer of silver perfluorocarboxylate is separated from the neighboring layer by twice the length of the perfluoroalkyl chain. The detailed assignments and interlayer d-spacings are summarized in Table 1. The averaged interlayer spacings are determined to be 33.54 ± 0.15, 38.87 ± 0.04, 44.29 ± 0.78, and 49.17 ± 0.18 Å for AgF12, AgF14, AgF16, and AgF18, respectively. The interlayer spacing versus $2n$ of each material is plotted in the inset of Figure 2. A linear relationship between the interlayer spacing and the chain length is observed. The slope is 1.30 ± 0.02 Å per $-CF_2-$ unit and the Y-intercept is 7.65 ± 0.47 Å. The linear correlation and thus the monotonic dependence of interlayer spacing with the number of perfluorocarbon units indicate that the materials share a common layered structure.

In the Ag K-EXAFS study of silver stearate, Tolochko et al.[17c] revealed that the silver atoms were bridged by the carboxylate in the form of dimers in an eight-membered ring,

TABLE 1: XRD Peaks and *d*-Spacings Derived from the (0*k*0) Reflections for $AgCO_2(CF_2)_nCF_3$

	AgF12		AgF14		AgF16		AgF18	
(0*k*0)	2θ	*d*(Å)	2θ	*d*(Å)	2θ	*d*(Å)	2θ	*d*(Å)
(010)								
(020)	5.28	16.74						
(030)	7.88	11.22	6.82	12.96	6.30	14.03	5.41	16.34
(040)	10.52	8.41	9.10	9.72	7.84	11.28	7.18	12.31
(050)	13.13	6.74	11.38	7.78	9.89	8.94	8.93	9.90
(060)	15.90	5.57	13.66	6.48	11.92	7.42	10.74	8.24
(070)	18.64	4.76	15.96	5.55	13.89	6.38	12.56	7.05
(080)			18.24	4.86	15.90	5.57	14.42	6.14
(090)			20.58	4.32	17.94	4.94	16.21	5.47
(0*10*0)			22.87	3.89	19.93	4.46	18.02	4.92
(0*11*0)			25.27	3.52	22.06	4.03	19.91	4.46
(0*12*0)					24.26	3.67	21.73	4.09
(0*13*0)					26.26	3.39	23.54	3.78
(0*14*0)							25.49	3.49
(0*15*0)							27.34	3.26

and the dimers were further bonded to each other by longer Ag−O bonds forming four-membered rings (see Figure 3). The bond lengths determined for silver stearate were r(Ag−Ag) = 2.90 Å, r(Ag−O) = 2.25 Å, r(C−O) = 1.20 Å, and r(−OO*C*−*C*H_2−) = 1.54 Å.[17c] On the other hand, according to the photographic X-ray study conducted by Blakeslee and Hoard,[20] the bond lengths in silver perfluorobutyrate are r(Ag−Ag) = 2.90 Å, r(Ag−O) = 2.24 Å, r(C−O) = 1.25 Å, and r(−OO*C*−*C*F_2−) = 1.54 Å. Using these values, the thickness of the silver carboxylate slab, i.e., $2t_1$ in Figure 3, is estimated to be 4.83 Å. Considering that the interlayer spacings derived from Figure 2, the thickness of the perfluorocarbon layer, i.e., $2t_2$ in Figure 3, is then 28.71, 34.04, 39.46, and 44.34 Å for AgF12, AgF14, AgF16, and AgF18, respectively.

By analyzing the XRD data, Bunn and Howells[21] concluded that the fluorocarbon chain in poly(tetrafluoroethylene) assumes a helical structure. This may not be unexpected since a fluorine atom is much larger than a hydrogen atom. The carbon backbone has a twisted zigzag conformation probably due to the steric hindrance of the fluorine atoms, thereby extending fully in a condensed state. The shape of the fluorocarbon chain thus looks like a circular cylinder in contrast to the flat cross-section of the planar zigzag hydrocarbon chains. It has to be mentioned that the slope determined from the inset of Figure 2 for silver perfluorocarboxylates, i.e., 1.30 Å, is exactly the same as the chain length per CF_2 group in poly(tetrafluoroethylene).[21] This implies that the perfluorocarbon chains in silver perfluorocarboxylates are also fully extended with their orientation being perpendicular to the Ag plane. Taking into account the fact that the van der Waals radius of the CF_3 group is 2.16 Å,[20,21] the chain length from the carboxylate carbon to the terminal $-CF_3$ group in silver perfluorocarboxylates should be 16.46 Å for AgF12, 19.06 Å for AgF14, 21.66 Å for AgF16, and 24.26 Å for AgF18. Doubling these values yields 32.92, 38.12, 43.32, and 48.52 Å, which results are 4.08 ± 0.14 Å longer than those derived from the measured XRD data, i.e., 28.71 Å for AgF12, 34.04 Å for AgF14, 39.46 Å for AgF16, and 44.34 Å for AgF18. Although the present estimate is prone to error resulting from the uncertainties in the slab thickness, the consistent difference, i.e., ∼4 Å, for all samples is remarkable. Recalling that the van der Waals diameter of a CF_3 group is 4.32 Å, this may indicate that the adjacent layers in silver perfluorocarboxylates overlap by as much as 94% of the terminal CF_3 groups. This is in sharp contrast with the cases for silver alkanoate and silver alkanethiolate. The extent of interpenetration has been reported to be as small as ∼1 Å for silver stearate[18b] and ∼0.5 Å for silver alkanethiolate.[16f] A fair extent of the penetration in silver perfluorocarboxylates must be attributed to the intrinsic nature of the fluorine atom. Although we cannot derive the intralayer structure due to the insufficient signal-to-noise ratio for high-angle XRD peaks, the overall structure of the silver perfluorocarboxylate as drawn in Figure 3 is presumably similar to that of silver hydroalkanecarboxylate.

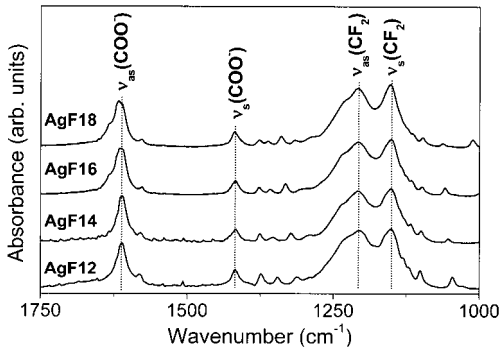

Figure 4. DRIFT spectra of $AgCO_2(CF_2)_nCF_3$.

TABLE 2: Characteristic IR Absorption Peaks for $AgCO_2(CF_2)_nCF_3$[a]

	ν_{as}(COO$^-$)	ν_s(COO$^-$)	$\Delta\nu$[b]	ν_{as}(CF$_2$)[c]	ν_s(CF$_2$)[c]
AgF12	1611	1418	193	1206	1151
AgF14	1612	1417	195	1207	1151
AgF16	1613	1418	195	1207	1151
AgF18	1613	1419	194	1208	1152

[a] Units in cm^{-1}. [b] ν_{as}(COO$^-$) − ν_s(COO$^-$). [c] Assigned based on refs 12c, 12e, 13b, and 13c.

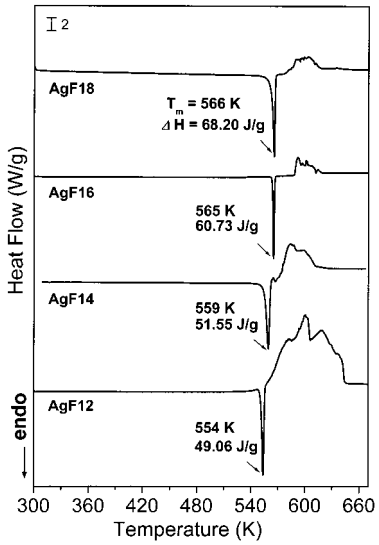

Figure 5. DSC traces of $AgCO_2(CF_2)_nCF_3$; the major transition temperatures and their associated enthalpies are denoted.

Figure 4 shows the DRIFT spectra of the silver perfluorocarboxylates. The observed peaks are summarized in Table 2. Regardless of the detailed composition, the characteristic IR bands are observed at the same positions, indicating that all the materials prepared in this work share a common structure, as revealed by the XRD analyses. The symmetric and antisymmetric CF_2 stretching peaks, i.e., $\nu_s(CF_2)$ and $\nu_{as}(CF_2)$, are clearly observed at 1151 and 1207 cm^{-1}, respectively. The symmetric and antisymmetric stretching peaks of the carboxylate group, i.e., $\nu_s(COO^-)$ and $\nu_{as}(COO^-)$, are also clearly identified at 1418 and 1612 cm^{-1}, respectively. However, the carbonyl stretching band (ν(C═O)) observable at ∼1700 cm^{-1} in free acids is completely absent, indicating that the obtained sample

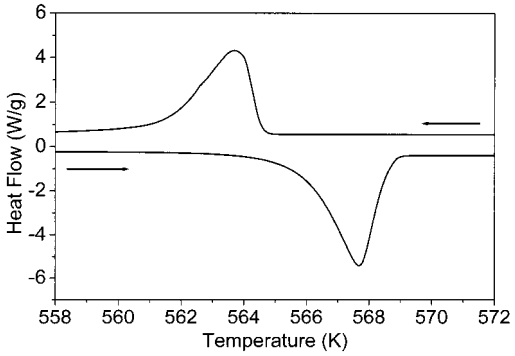

Figure 6. DSC traces for heating (lower) and cooling (upper) cycles of AgF18.

is not contaminated with free acid. Referring to the empirical relationship between the frequency difference, $\Delta\nu = \nu_{as}(COO^-) - \nu_s(COO^-)$, and the type of bonding,[22,23] the binding state of the carboxylate group to silver is presumed to be a bridging one.

One of the purposes of this work was to compare the thermal characteristics of perfluorocarboxylates with those of hydroalkanoates. We thus conducted DSC, TGA, and variable-temperature XRD measurements. The DSC traces of AgF12, AgF14, AgF16, and AgF18 are shown in Figure 5. It is clear that an endothermic phase transition occurs sharply at 554−566 K for all samples; both the transition temperature and the endothermic enthalpy increase slightly as a function of the chain length. This endothermic transition is presumably associated with the chain melting process of the fluorocarbon moiety. The transition is also presumed to be reversible because the exothermic transition enthalpy on cooling after heating to 572 K (ΔH_{cool}) is almost the same as the endothermic one (ΔH_{heat}); see for instance the cyclic DSC traces of AgF18 in Figure 6. We can also identify from Figure 5 that a rather complex exothermic transition takes place immediately after the sharp endothermic transition. This phenomenon can be ascribed to the decomposition of the silver perfluorocarboxylate (vide infra).

Figure 7 shows the TGA and its first derivative traces recorded for four different samples. The major mass loss occurs around ∼600 K for all samples. On the basis of the molecular weight of silver perfluorocarboxylates ($AgCO_2(CF_2)_nCF_3$), the actual mass loss amounts to the nearly complete loss of the organic moiety ($CF_3(CF_2)_nCOO-$) from the parent material. This can be seen from Table 3 although there is a fair amount of discrepancy for AgF12. The final residual mass can then be attributed to metallic silver, which is separately confirmed by the variable-temperature XRD measurements (vide infra). Much the same observations were made by Szłyk et al.[24] for the Ag(I) salts of fluorinated carboxylic and sulfonic acids. On the basis of the TGA measurements, they also concluded that $CF_3(CF_2)_6COO-$ (or $CF_3(CF_2)_8COO-$), for instance, was detached from $CF_3(CF_2)_6COOAg$ (or $CF_3(CF_2)_8COOAg$), leaving metallic silver as the final decomposition product.

TABLE 3: Observed and Calculated Mass Loss for $AgCO_2(CF_2)_nCF_3$

		M_{obs} (M_{cal})[b]	
	T (K)[a]	$CF_3(CF_2)_nCOO$	Ag
AgF12	603	70.47 (85.04)	29.53 (14.96)
AgF14	600	86.76 (86.86)	13.24 (13.14)
AgF16	602	87.88 (88.29)	12.12 (11.71)
AgF18	605	89.79 (89.44)	10.21 (10.56)

[a] Peak temperature observed in the first derivative of TGA trace. [b] Observed and calculated % mass loss.

To obtain further information on the thermal behavior of silver perfluorocarboxylates, we have performed variable-temperature XRD measurements. Figure 8 shows a series of X-ray diffractograms taken for AgF18 as a function of temperature. All diffractograms were obtained at the temperatures indicated, with the temperature held constant to ±1 K. The temperature was raised from 303 to 573 K in 10 K steps. A well-developed progression of intense reflections is invariably seen up to 553 K. This indicates that the bilayer structural motif is sustained up to the temperature. Upon increasing the temperature, the XRD peaks indexed as (0*k*0) abruptly decrease from 563 K and become completely absent above 573 K. Instead, two new peaks are identified at 37.7 and 43.9° which can be assigned, respectively, to the (111) and (200) reflections of metallic silver.[25] These features indicate that a chain-melting process commences at ∼560 K for silver perfluorocarboxylate but immediately the layered structure is collapsed to produce metallic silver. Hence, the XRD observations are comparable to the DSC and TGA observations. We found separately that

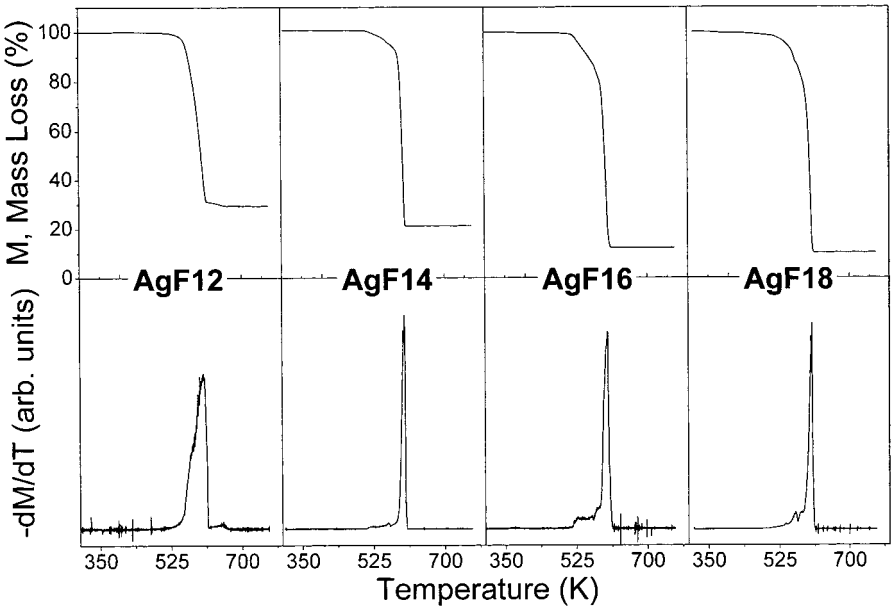

Figure 7. TGA (top) and its first derivative (bottom) traces for $AgCO_2(CF_2)_nCF_3$.

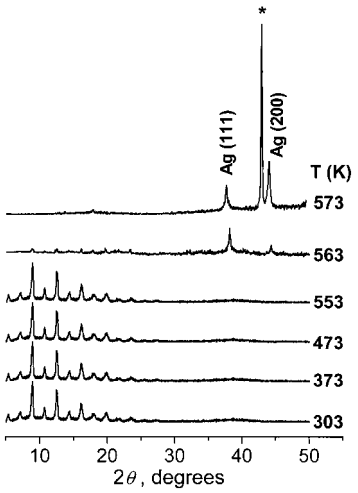

Figure 8. Variable-temperature XRD patterns for AgF18. Reflections from the metallic silver are marked in the topmost diffractogram. The peak labeled with asterisk (*) is due to the base plate.

the thermal decomposition products at 573 K (in an atmosphere of N_2) consisted of highly monodisperse perfluorocarbon-stabilized silver nanoparticles; the average diameter of the nanoparticles was ~5 nm regardless of the perfluorocarbon chain length.[26] The possible mechanism of the formation of nanoparticles is a matter of conjecture at the moment, and its elucidation thus remains as one of our future research subjects.

The thermal characteristics of silver perfluorocarboxylate are in sharp contrast to those of silver hydroalkanoate. As mentioned in the Introduction, for a typical silver hydroalkanoate, i.e., silver stearate, structural changes take place in two temperature regions.[18b] In the first transition at ~380 K, the binding state of carboxylate is converted from bridging to unidentate. Although the alkyl chains are also subjected to considerable disordering (premelting event), the layered structural motif is nonetheless sustained; hence, the overall structural change is partially irreversible. In the second transition at ~500 K, a totally irreversible structural change takes place, that is, the decomposition of silver stearate. Unlike in the case of silver stearate, for silver perfluorocarboxylate a chain melting process commences at ~560 K without any interim premelting event; although not shown here, the DRIFT spectral feature was also similarly invariant up to ~560 K as seen in the XRD measurements. This implies that the binding state of the carboxylate group to silver, a bridging one, is maintained up to ~560 K for silver perfluorocarboxylates. As mentioned above, for silver stearate, the conversion from bridging to unidentate state occurs merely around ~380 K. The invariable binding state of carboxylate groups in silver perfluorocarboxylates must be associated with the high rigidity of the fluorocarbon chain. Without premelting event, the motion of fluorocarbons will be very limited such that there is no room for carboxylate groups to transform from bridging to unidentate state. Another noteworthy difference is that, for silver perfluorocarboxylates, the thermal decomposition reactions takes place immediately after the chain melting process. Accordingly, the temperature at which the structural collapse occurs is ~100 K higher in silver perfluorocarboxylate than in silver stearate. The enhanced thermal stability of the silver perfluorocarboxylate must also be associated with the high rigidity of the fluorocarbon chain. Hence, it will be beneficial to incorporate perfluorocarbons as the organic moiety when it is desired to manufacture thermally stable organic/inorganic hybrid materials.

4. Conclusion

The platelets observed in the SEM image of the silver perfluorocarboxylates were identified by XRD measurements to possess a layered structure similarly to silver hydroalkanoate. The interlayer spacings estimated from the XRD data indicated that the perfluoro chains interpenetrated to a greater extent between the adjacent layers than the alkyl chains in silver hydroalkanoate or in silver alkanethiolate. The variable-temperature XRD and DRIFT measurements as well as the TG and DSC analyses revealed that for silver perfluorocarboxylate, a chain melting process proceeded without any premelting event but a thermal decomposition reaction followed immediately. This thermal behavior is also in sharp contrast to that in silver hydroalkanoates such as silver stearate. In addition, the temperature at which the structural collapse occurs is much higher than that for silver stearate. The enhanced thermal stability must be associated with the high rigidity of the perfluoro chain. The stability is one of the key factors for the organic materials to be applied in the technologically relevant fields. From the application aspect, perfluorocarbons will thus be a promising organic moiety to be incorporated in layered organic/inorganic hybrid materials.

Acknowledgment. This work was supported in part by the Ministry of Information and Communication (IMT-2000, 01-PJ11-PG9-01NT00-0023) and the Korea Science and Engineering Foundation (KOSEF, R03-2001-00021 and 1999-2-121-001-5). S.W.H. was also supported by KOSEF through the Center for Molecular Catalysis at Seoul National University. S.J.L. and H.J.C. are recipients of the BK21 fellowship.

References and Notes

(1) Chidsey, C. E. D.; Loiacono, D, N. *Langmuir* **1990**, *6*, 682.
(2) Schönherr, H.; Ringsdorf, H. *Langmuir* **1996**, *12*, 3891.
(3) Schönherr, H.; Ringsdorf, H.; Jaschke, M.; Butt, H. J.; Bamberg, E.; Allinson, H.; Evans, S. D. *Langmuir* **1996**, *12*, 3898.
(4) Miura, Y. F.; Takenaga, M.; Koini, T.; Graupe, M.; Garg, N.; Graham, R. L., Jr.; Lee, T. R. *Langmuir* **1998**, *14*, 5821.
(5) Tsao, M.-W.; Rabolt, J. F.; Schönherr, H.; Castner, D. G. *Langmuir* **2000**, *16*, 1734.
(6) Whitesides, G. M.; Laibinis, P. E. *Langmuir* **1990**, *6*, 87.
(7) Laibinis, P. E.; Whitesides, G. M. *J. Am. Chem. Soc.* **1992**, *114*, 1990.
(8) Ramos, L.; Weitz, D. A. *Langmuir* **2001**, *17*, 2275.
(9) Alves, C. A.; Porter, M. D. *Langmuir* **1993**, *9*, 3507.
(10) Liu, G.; Fenter, P.; Chidsey, C. E. D.; Ogletree, D. F.; Eisenberger, P.; Salmeron, M. *J. Chem. Phys.* **1994**, *101*, 4301.
(11) Garbassi, F.; Morroca, M.; Occhiello, E. *Polymer Surfaces*; Wiley: Chichester, U.K., 1994.
(12) (a) Tsao, M.-W.; Hoffmann, C. L.; Rabolt, J. F.; Johnson, H. E.; Castner, D. G.; Erdelen, C.; Ringsdorf, H. *Langmuir* **1997**, *13*, 4317. (b) Kato, T.; Kameyama, M.; Ehara, M.; Iimura, K. *Langmuir* **1998**, *14*, 1786. (c) Ha, K.; Ahn, W.; Rho, S.; Suh, S.; Synn, D.; Stelzle, M.; Rabolt, J. F. *Thin Solid Films* **2000**, *372*, 223. (d) Tamada, K.; Ishida, T.; Knoll, W.; Fukushima, H.; Colorado, R., Jr.; Graupe, M.; Shmakova, O. E.; Lee, T. R. *Langmuir* **2001**, *17*, 1913. (e) Ren, Y.; Iimura, K.; Ogawa, A.; Kato, T. *J. Phys. Chem. B* **2001**, *105*, 4305.
(13) (a) Fukushima, H.; Seki, S.; Nishikawa, T.; Takiguchi, H.; Tamada, K.; Abe, K.; Colorado, R., Jr.; Graupe, M.; Shmakova, O. E.; Lee, T. R. *J. Phys. Chem. B* **2000**, *104*, 7417. (b) Ren, Y.; Iimura, K.; Kato, T. *J. Chem. Phys.* **2000**, *113*, 1162. (c) Ren, Y.; Asanuma, M.; Iimura, K.; Kato, T. *J. Chem. Phys*. **2001**, *114*, 923.
(14) Kim, N.; Shin, S. *J. Chem. Phys.* **1999**, *111*, 6556.
(15) Naud, C.; Calas, P.; Commeyras, A. *Langmuir* **2001**, *17*, 4851.
(16) (a) Dance, I. G.; Fisher, K. J.; Bamda, R. M. H.; Scudder, M. L. *Inorg. Chem.* **1991**, *30*, 183. (b) Baena, M. J.; Espinet, P.; Lequercia, M. C.; Levelut, A. M. *J. Am. Chem. Soc.* **1992**, *114*, 4182. (c) Fijolek, H. G.; Grohal, J. R.; Sample, J. L.; Natan, M. J. *Inorg. Chem.* **1997**, *36*, 622. (d) Bensebaa, F.; Ellis, T. H.; Kruss, E.; Voicu, R.; Zhou, Y. *Can. J. Chem.* **1998**, *76*, 1654. (e) Bensebaa, F.; Ellis, T. H.; Kruus, E.; Voicu, R.; Zhou, Y. *Langmuir* **1998**, *14*, 6579. (f) Parikh, A. N.; Gillmor, S. D.; Beers, J. D.; Beardmore, K. M.; Cutts, R. W.; Swanson, B. I. *J. Phys. Chem. B* **1999**,

103, 2850. (g) Bardeau, J. F.; Parikh, A. N.; Beers, J. D.; Swanson, B. I. *J. Phys. Chem. B* **2000**, *104*, 627.

(17) (a) Vand, A.; Atkins, A.; Cambell, R. K. *Acta Cryst*. **1949**, *2*, 398. (b) Matthews, F. W.; Warren, G. G.; Michell, J. H. *Anal. Chem.* **1950**, *22*, 514. (c) Tolochko, B. P.; Chernov, S. V.; Nikitenko, S. G.; Whitcomb, D. R. *Nucl. Instrum. Methods A* **1998**, *405*, 428.

(18) (a) Lee, S. J.; Han, S. W.; Choi, H. J.; Kim, K. *Eur. Phys. J. D* **2001**, *16*. 293. (b) Lee, S. J.; Han, S. W.; Choi, H. J.; Kim, K. *J. Phys. Chem. B* **2002**, *106*, 2892.

(19) (a) Aksay, I. A.; Trau, M.; Manne, S.; Honma, I.; Yao, N.; Zhou, L.; Fenter, P.; Eisenberger, P. M.; Gruner, S. M. *Science* **1996**, *273*, 892. (b) Lacroix, P. G.; Clement, R.; Nakatani, K.; Zyss, J.; Ledoux, I. *Science* **1994**, *263*, 658. (c) Vermeulen L. A.; Thompson, M. E. *Nature* **1992**, *358***,** 656. (d) Laget, V.; Hornick, C.; Rabu, P.; Drillon, M.; Turek, P.; Ziessel, R. N. *Adv. Mater*. **1998**, *10***,** 1024.

(20) Blakeslee, A. E.; Hoard, J. L. *J. Am. Chem. Soc*. **1956**, *78*, 3029.

(21) Bunn, C. W.; Howells, E. R. *Nature* **1954**, *174*, 549.

(22) Lee, S. J.; Han, S. W.; Yoon, M.; Kim, K. *Vib. Spectrosc.* **2000**, *24*, 265.

(23) (a) Gericke, A.; Hühnerfuss, H. *Thin Solid Films* **1994**, *245*, 74. (b) Ohe, C.; Ando, H.; Sato, N.; Urai, Y.; Yamamoto, M.; Itoh, K. *J. Phys. Chem. B* **1999**, *103*, 435.

(24) Szłyk, E.; Łkomska, I.; Grodzicki, A. *Thermochim. Acta* **1999**, *223*, 207.

(25) JCPDS ICDD PDF No. 02-1098, 03-0921, 03-0931.

(26) Lee, S. J.; Han, S. W.; Kim, K. *Chem. Commun.* **2002**, 442.